Shell Erosion and Shape Coexistence in $^{43}_{16}$S$_{27}$

L. Gaudefroy,[1,*] J. M. Daugas,[1] M. Hass,[2] S. Grévy,[3] Ch. Stodel,[3] J. C. Thomas,[3] L. Perrot,[4] M. Girod,[1] B. Rossé,[1]
J. C. Angélique,[5] D. L. Balabanski,[6] E. Fiori,[7] C. Force,[3] G. Georgiev,[7] D. Kameda,[8] V. Kumar,[2] R. L. Lozeva,[7] I. Matea,[9]
V. Méot,[1] P. Morel,[1] B. S. Nara Singh,[10] F. Nowacki,[11] and G. Simpson[5]

[1]*CEA, DAM, DIF, F-91297 Arpajon, France*
[2]*The Weizmann Institute, 76100 Rehovot, Israel*
[3]*GANIL, CEA/DSM - CNRS/IN2P3, F-14076 Caen, France*
[4]*IPN, IN2P3-CNRS, F-91406 Orsay, France*
[5]*LPSC, F-38026 Grenoble, France*
[6]*Faculty of Physics, University of Sofia, BG-1164 Sofia, Bulgaria*
[7]*CSNSM, F-91404 Orsay, France*
[8]*RIKEN, 2-1 Hirosawa, Wako, Saitama 351-0198, Japan*
[9]*CENBG, UMR 5797 CNRS/IN2P3, Université Bordeaux 1, F-33175 Gradignan, France*
[10]*Department of Physics, University of York, YO 10 5DD York, United Kingdom*
[11]*IPHC, IN2p3-CNRS, F-67037 Strasbourg, France*

We report on the g-factor measurement of the first isomeric state in $^{43}_{16}$S$_{27}$ [$E_x = 320.5(5)$ keV, $T_{1/2} = 415(5)$ ns, and $g = 0.317(4)$]. The $7/2^-$ spin-parity of the isomer and the intruder nature of the ground state of the nucleus are experimentally established for the first time, providing direct and unambiguous evidence of the collapse of the $N = 28$ shell closure in neutron-rich nuclei. The shell model, beyond the mean-field and semiempirical calculations, provides a very consistent description of this nucleus showing that a well deformed prolate and quasispherical states coexist at low energy.

The determination of electromagnetic moments is of broad interest in subatomic physics: (i) the magnetic moment of the muon provides an important test of the standard model [1,2]; (ii) the anomalous magnetic moments of nucleons, first thought as elementary constituents of the atomic nucleus, are a fingerprint of the quark subnucleonic degree of freedom [3,4]; and (iii) the discovery of the nonvanishing electric quadrupole moment of the deuteron [5] was the first evidence for the need of a tensor term in the nuclear interaction [6].

In nuclear physics, thanks to recent experimental developments, electromagnetic moments can now be determined with a high precision [7,8]. Measurements of g-factors constrain our understanding of nuclear structure far from the stability line because of the large difference between the proton and neutron magnetic moments ($\mu_\nu/\mu_\pi \simeq -2/3$). Recent intense experimental and theoretical interest has been devoted to the study of the evolution of nuclear structure around the $N = 28$ shell closure [9,10]. Even though not firmly ascertained yet, the present understanding is that the spherical $N = 28$ shell gap is progressively eroded when moving away from the stability line so that deformation takes place [9]. Among the $N = 27$–28 isotones, sulfur ones are of particular interest since shape coexistence is expected to occur [11–14]. More specifically, the occurrence of the low-lying isomer at 319 keV in ^{43}S$_{27}$ [13] has been interpreted in the shell model (SM) framework as resulting from the inversion between the natural $(\nu f_{7/2})^{-1}$ and the intruder $(\nu p_{3/2})^{+1}$

configurations [10,13]. In this Letter, we report on the g-factor measurement of this isomer using the Time Dependent Perturbed Angular Distribution (TDPAD) method [7]. The present results provide the first unambiguous experimental evidence of the collapse of the $N = 28$ shell closure in neutron-rich nuclei. Results of SM, beyond the mean field and semiempirical calculations are also reported to consistently show that the low-lying structure of ^{43}S is driven by the coexistence of deformed and quasispherical states.

The ^{43m}S nuclei were produced and spin-oriented via the fragmentation of a $60A \cdot$ MeV $^{48}Ca19+$ primary beam (mean intensity of 1 μAe). It impinged on a 535 μm Be target, located at the entrance of the LISE-2000 spectrometer at GANIL [15]. A wedge degrader of 465 μm of Be was used at the first dispersive plane of the spectrometer to avoid contamination from other species in the beam. The detection setup was located at the focal point of the spectrometer, at about 20 m distance from the production target. The time of flight through the spectrometer for ^{43}S was about 200 ns. Within this experimental configuration, about 75% out of the produced ^{43m}S isomers reached the detection system for g-factor measurement. A 50 μm thick plastic scintillator provided a start signal for the TDPAD measurement and was placed about 1 m upstream from an annealed high-purity 1 mm thick Cu host. The Cu host was placed between the poles of an electromagnet providing a constant magnetic field $\vec{B}$ in the vertical direction. It was used to induce a Larmor precession of the spin-aligned

^{43m}S nuclei, implanted in the catcher. Four coaxial Ge detectors were positioned in the horizontal plane around the host at 90° with respect to each other. The left part of Fig. 1 shows a schematic view of the experimental setup and the right part displays the energy spectrum of the γ-rays collected during this experiment. The most intense γ-ray at 320.5(5) keV is associated with the ^{43m}S decay.

The time interval between an event in the plastic scintillator and a signal in one of the four Ge detectors was recorded on an event-by-event basis. It was used to reconstruct the time pattern associated to the 320.5(5) keV line for each detector. These patterns were combined to generate the $R(t)$ function associated with the γ line:

$$R(t) = \frac{I_{12}(\theta, t) - \epsilon I_{34}(\theta + \pi/2, t)}{I_{12}(\theta, t) + \epsilon I_{34}(\theta + \pi/2, t)}$$
$$\propto \cos[2(\omega_L t + \alpha - \theta)], \tag{1}$$

where $I_{ij}(\theta, t)$ is the photopeak intensity in Ge detectors i and j (see Fig. 1), at time t; θ is the angle between the beam axis and the pair of Ge detectors 1 and 2; ϵ is a normalization coefficient. The precession frequency is defined by $\omega_L = -g\mu_N B/\hbar$. The angle α accounts for the rotation of the nuclear spin during the recoil separation in the spectrometer. To reduce systematic errors, two measurements of the g-factor have been performed at two magnetic field intensities: $B_1 = 0.275(2)$ T and $B_2 = 0.688(4)$ T, measured with a Hall probe. Error bars in these intensities account for field inhomogeneities along the beam spot size ($\varnothing \simeq 5$ mm) at the implantation point. The deduced $R(t)$ functions presented in Fig. 2 for both magnetic fields are in a very good agreement. The weighted mean value of the g-factor for the ^{43m}S state is $g = -0.317(4)$. The uncertainty stated here includes the statistical uncertainty and the uncertainty of the magnetic field. This g-factor can only be reproduced by a single neutron in the $\nu f_{7/2}$ orbit ($g_{Schmidt} = -0.546$) which suggests a spin-parity assignment $J^\pi = 7/2^-$ for the state. Note that a single neutron in the $\nu p_{3/2}$ orbit gives $g_{Schmidt} = -1.274$, while a single

neutron in other fp orbits would give rise to a positive g-factor.

A relation similar to that of the $R(t)$ function can be obtained to cancel out the effect of the Larmor precession in the collected time patterns, allowing one to deduce the half-life of the 320.5(5) keV state with a much better precision than previously known [13]: $T_{1/2} = 415(5)$ ns. Such a half-life unambiguously points towards the multipolarity $\lambda = 2$ for the 320.5(5) keV transition. A $\lambda = 1(3)$ transition would lead to a much shorter (longer) half-life. The magnetic nature ($M2$) of the transition can be excluded because it would imply nucleon excitations from sd to fp shells expected at much higher energy [9] requiring a longer half-life for the isomer. From energetic arguments and selection rules for $E2$ transitions, the spin-parity of the ground state (GS) of ^{43}S is deduced to be $J^\pi = 3/2^-$. Such a J^π value is accounted for by neutron excitation across the $N = 28$ gap. This result firmly establishes the erosion of the $N = 28$ gap in exotic nuclei.

Shell model calculations have been performed using the ANTOINE code [16,17] and the up-to-date $sdpf$ interaction [18]. The valence space was restricted to sd (fp) orbits for protons (neutrons). Using free nucleon g-factors, the gyromagnetic factor of the isomer, calculated at 700 keV, is $g = -0.280$, in a very good agreement with our value. However, it is well known that spin quenching and orbital enhancement are to be considered leading to renormalization of nucleon g-factors [19]. Using the adopted values for these latter in the $sdpf$ valence space ($g_\ell^\pi = 1.1$, $g_s^\pi = 4.1895$, $g_\ell^\nu = -0.1$, and $g_s^\nu = -2.8695$) leads to $g = -0.269$, still in good agreement with our experimental value. Admixtures of spin-flip configurations ($\nu f_{7/2} - \nu f_{5/2}$ or $\pi d_{5/2} - \pi d_{3/2}$) in the wave function of the isomer are found to account for the departure of the g-factor from its Schmidt value [20].

The $E2$ transition probability between the $7/2_1^-$ state and the GS is calculated to be $1.4\ e^2 \cdot$ fm^4 (using $0.35e$ and $1.35e$ as effective charges for neutrons and protons [18], respectively). This value is consistent with that deduced

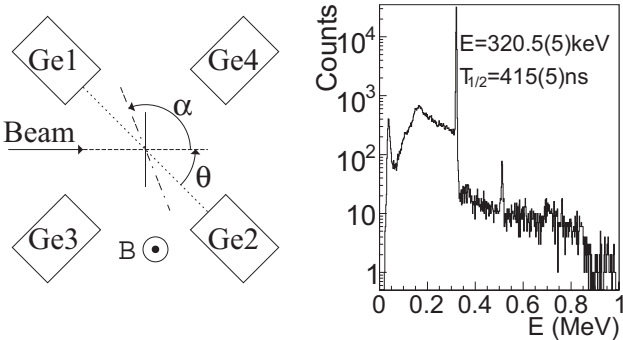FIG. 1.   Left: Outline of the experimental setup. The dashed-dotted line shows the orientation of the spin of the ^{43m}S state at $t = 0$. α and θ are defined in the text. Right: Full statistics γ-ray spectrum obtained in the present work.
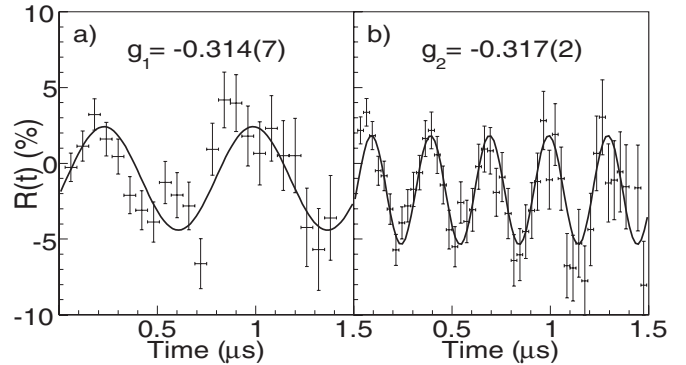

FIG. 2. $R(t)$ functions associated with the 320.5 keV γ-ray for (a) the magnetic field B_1 and (b) B_2. Solid curves display the result of the fit using the $R(t)$ function from Eq. (1).

from our experimental work [$B(E2 \downarrow) = 0.403(8)$ $e^2 \cdot$ fm^4]. The origin of the hindrance factor (20) associated with this small $B(E2 \downarrow)$ value is discussed in the following.

SM calculations have been extended to higher excited states in ^{43}S to look for deformed structures expected in this mass region [10–14]. As shown in Fig. 3, a $K = 1/2$ decoupled rotational band is calculated with the following characteristic features: (i) along the band, the intrinsic charge quadrupole moment ($Q_0^{SM} \simeq 65$ $e \cdot$ fm^2) of the states is constant within 10%; (ii) states differing by two units of total angular momentum (TAM) are linked by strong $E2$ transitions (black arrows in Fig. 3); (iii) states differing by 1 unit of TAM are linked by strong $M1$ transitions (white arrows in Fig. 3); and (iv) other electromagnetic transitions contribute with a negligible rate. The $7/2_2^-$ state belonging to the band, calculated at 1.00 MeV, probably corresponds to the state at 940 keV reported in Ref. [21] ($7/2_2^-$ state shown in the experimental level scheme of Fig. 3), given the good agreement on excitation energy and $B(E2)$ values.

The aforementioned features are typically those encountered in axially deformed nuclei. Within this assumption, a large deformation parameter ($\beta^{SM} = 0.30$) is deduced for the GS from the relation: $Q_0^{SM} = \frac{3}{\sqrt{5\pi}} Z(r_0 A^{1/3})^2 \beta^{SM}(1 + \sqrt{\frac{5}{64\pi}} \beta^{SM})$, using $r_0 = 1.20$ fm and the quadrupole moment obtained from SM calculations. The structure of axially deformed nuclei is usually well accounted for by the particle-plus-rotor (PR) model [22]. Indeed, using $\hbar^2/2\mathcal{J} = 109$ keV as inertia parameter, and $a = -1.384$ as decoupling parameter, one obtains remarkable agreement between PR and SM calculations as shown in the left part of Fig. 3. Moreover, as shown in the insert of Fig. 3, the magnetic moments calculated in the SM framework follow to better than 20% the expectation values of the PR model obtained using $g_R = 0.08$ as rotational moment, $g_K =$

-0.968 as intrinsic moment and $b_0 = 1.89$ as magnetic decoupling parameter. We note that the present value of the rotational moment is far from that conventionally observed ($g_R = Z/A$) in heavier nuclei. As already discussed in detail in Ref. [23], it stems from the important neutron contribution to the wave function of the states of the rotational band. The global coherence between the PR and SM models confirms the $K = 1/2$ nature of the GS band in ^{43}S with an axially symmetric shape. Both the low $B(E_2 : 7/2_1^- \rightarrow 3/2_{GS}^-)$ value reported here and the absence of calculated deformed structure built on the $7/2_1^-$ isomer suggest a coexistence of different shapes in the low-lying structure of the nucleus. The SM results reported in Ref. [10] support this conclusion. They show that correlation energy is much lower in the $7/2_1^-$ state than in the GS of ^{43}S. They also support the configuration inversion and the large deformation parameter deduced here.

In confirmation to the present results on ^{43}S, constrained mean-field Hartree-Fock-Bogolyubov (HFB) and beyond the mean-field calculations have been performed in axial symmetry using the Gogny D1S effective force [24]. The blocking technique has been used to treat the unpaired neutron in HFB calculations. The resulting potential energy curves (including zero point energy corrections [25]) are drawn as a function of the deformation parameter (β) in Fig. 4. The unpaired neutron has been blocked in the magnetic states of either the $\nu f_{7/2}$ (opened symbols in Fig. 4) or the $\nu p_{3/2}$ (filled symbols in Fig. 4) orbit. The curve corresponding to the $K = 3/2$ magnetic state originating from the $\nu p_{3/2}$ orbit stands at higher energy and is not reported in the figure. The generator coordinate method (GCM) within the Gaussian overlap approximation (GOA) has been applied to perform configuration mixings of HFB states [25]. The resulting states are shown inside the gray boxes in Fig. 4. Positions of these boxes give the energy and mean β-deformation of the states. One finds a strik-
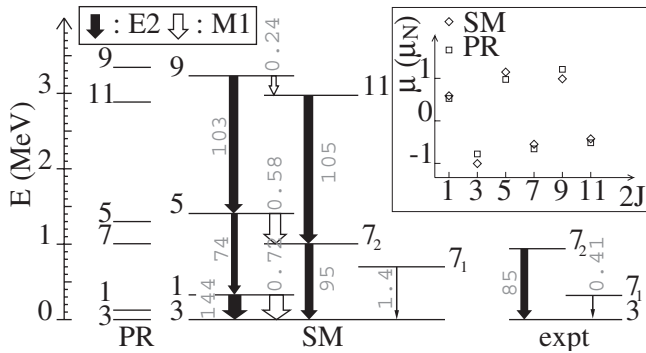

FIG. 3. Experimental (expt) level scheme of ^{43}S, compared to SM and PR models. The states, of negative parity, are labeled by twice their spin value. Transition probabilities [in $e^2 \cdot$ fm^4 (μ_N) for $E2$ ($M1$) transitions] are reported along the arrows. Arrow width is proportional to the strength of the transition. The insert compares PR and SM predictions for the magnetic moments of the states of the rotational band.
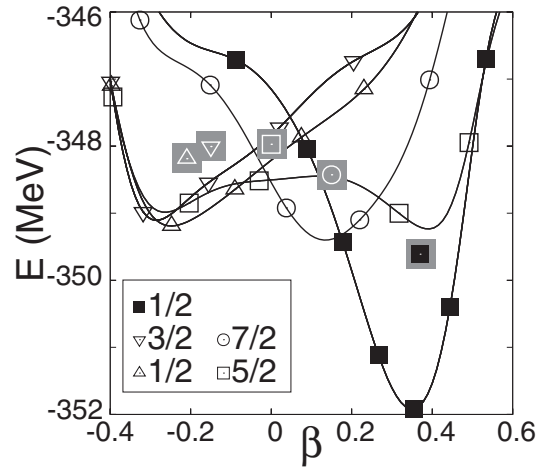

FIG. 4. HFB potential energy curves with zero-point energy corrections for the first blocked states in ^{43}S. States are labeled by their K values (see text for details).

ingly good agreement between GCM + GOA and SM approaches. Indeed, the former calculations also predict a $K = 1/2$ GS, originating from the $\nu p_{3/2}$ orbit, with a deformation parameter $\beta^{MF} = 0.37$ and a mean-charge quadrupole moment $Q_0^{MF} = 65 \; e \cdot fm^2$. The calculated inertia parameter ($\hbar^2/2\mathcal{J} = 119$ keV) and decoupling parameter ($a = -1.126$) are also in close agreement with PR results. The four K-components originating from the $\nu f_{7/2}$ orbital are found to lie within 400 keV only. One has to note that projection on the total angular momentum (J) has not been included in the present GCM + GOA calculations. Given the broadness of the HFB potential energy curves (Fig. 4), the physical states resulting from such a projection are likely to mix with each other, especially the $K = 5/2$ and $K = 7/2$ components that are close both in energy and β-deformation. Thus, one might expect that the physical $7/2_1^-$ state in ^{43}S lies in the range $0 \le \beta \le 0.15$.

The various and complementary theoretical approaches (PR, SM, or GCM + GOA) used here, combined with the presented experimental results, provide a remarkably consistent picture of the low-lying structure of ^{43}S: coexistence of noninteracting deformed ground and quasispherical isomeric states occurs. It accounts for the large hindrance factor of the $7/2_1^- \rightarrow 3/2_{gs}^-$ transition. The situation significantly differs in ^{44}S, where both the deformed and spherical configurations are predicted to coexist [11] *and* to be well mixed [12], as supported by the observation of the low-lying 0_2^+ state at 1.365 MeV [14]. In the SM framework, this state is calculated 1.220 MeV above the 0_{gs}^+. The parentages [i.e., the spectroscopic factors (SFs)] between these 0^+ states in ^{44}S and the $3/2_1^-$ and $7/2_1^-$ states in ^{43}S are found to be important: $SF(0_1^+ \rightarrow 3/2^-) \simeq SF(0_2^+ \rightarrow 3/2^-) \simeq 0.5$ and $SF(0_1^+ \rightarrow 7/2^-) \simeq 2SF(0_2^+ \rightarrow 7/2^-) \simeq 0.4$. Such large spectroscopic factors show that the wave functions of both the 0^+ states in ^{44}S are an almost equivalent mixing of both prolate and quasispherical configurations encountered in ^{43}S, in agreement with Ref. [12]. In conclusion, the gyromagnetic factor of the $7/2_1^-$ isomer in ^{43}S, at 320.5(5) keV, has been measured using the TDPAD method. The reported g-factor proves that this excited state is built on the $\nu f_{7/2}$ orbit. The experimental evidence for a $\nu p_{3/2}$ ground state substantiates the erosion of the $N = 28$ shell gap, strongly supported by SM calculations. Within this theoretical approach, the ground state of ^{43}S is found to be part of a well deformed ($\beta = 0.30$) $K = 1/2$ decoupled rotational band. The isomeric state is shown not to belong to this band and to have a rather spherical shape. These SM based conclusions are in a very good agreement and nicely complemented by GCM + GOA calculations using the Gogny D1S force, as well as by semiempirical calculations. Further experimental and theoretical efforts would be of interest to better understand the sudden onset of collectivity in neutron-rich nuclei around $N = 28$.

*laurent.gaudefroy@cea.fr

[1] R. M. Carey *et al.*, Phys. Rev. Lett. **82**, 1632 (1999).
[2] H. N. Brown *et al.*, Phys. Rev. Lett. **86**, 2227 (2001).
[3] L. W. Alvarez and F. Bloch, Phys. Rev. **57**, 111 (1940).
[4] J. Weyers, Phys. Rev. Lett. **18**, 1033 (1967).
[5] J. M. B. Kellogg *et al.*, Phys. Rev. **55**, 318 (1939).
[6] H. A. Bethe, Phys. Rev. **55**, 1261 (1939).
[7] G. Neyens, Rep. Prog. Phys. **66**, 633 (2003).
[8] N. Benczer-Koller and G. J. Kumbartzki, J. Phys. G **34**, R321 (2007).
[9] O. Sorlin and M.-G. Porquet, Prog. Part. Nucl. Phys. **61**, 602 (2008) and references therein.
[10] L. Gaudefroy *et al.*, Phys. Rev. C **78**, 034307 (2008).
[11] S. Péru, M. Girod, and J. F. Berger, Eur. Phys. J. A **9**, 35 (2000).
[12] E. Caurier, F. Nowacki, and A. Poves, Nucl. Phys. A **742**, 14 (2004).
[13] F. Sarazin *et al.*, Phys. Rev. Lett. **84**, 5062 (2000).
[14] S. Grévy *et al.*, Eur. Phys. J. A **25**, 111 (2005).
[15] R. Anne *et al.*, Nucl. Instrum. Methods Phys. Res., Sect. A **257**, 215 (1987).
[16] E. Caurier, ANTOINE code, IReS, Strasbourg 1989–2002.
[17] E. Caurier and F. Nowacki, Acta Phys. Pol. B **30**, 705 (1999).
[18] F. Nowacki and A. Poves, Phys. Rev. C **79**, 014310 (2009).
[19] E. Caurier *et al.*, Rev. Mod. Phys. **77**, 427 (2005).
[20] H. Noya, A. Arima, and H. Horie, Prog. Theor. Phys. **8**, 33 (1958).
[21] R. W. Ibbotson, T. Glasmacher, P. F. Mantica, and H. Scheit, Phys. Rev. C **59**, 642 (1999).
[22] A. Bohr and B. R. Mottelson, *Nuclear Structure* (Benjamin, New York, 1975), Vol. II.
[23] A. D. Davies *et al.*, Phys. Rev. Lett. **96**, 112503 (2006); A. E. Stuchbery *et al.*, Phys. Rev. C **74**, 054307 (2006).
[24] J.-F. Berger, M. Girod, and D. Gogny, Comput. Phys. Commun. **63**, 365 (1991).
[25] J. Libert, M. Girod, and J.-P. Delaroche, Phys. Rev. C **60**, 054301 (1999).